ELSEVIER

International Journal of Mass Spectrometry 205 (2001) 233–242

International Journal of Mass Spectrometry

Dissociative charge transfer from highly excited Na Rydberg atoms to vibrationally excited Na_2 molecules

Oliver Kaufmann[a], Aigars Ekers[a,b]*, Christian Gebauer-Rochholz[a], Kai Uwe Mettendorf[a], Matthias Keil[a] and Klaas Bergmann[a]

[a]*Fachbereich Physik der Universität Kaiserslautern, D-67653 Kaiserslautern, Germany*
[b]*University of Latvia, Institute of Atomic Physics and Spectroscopy, LV-1586 Riga, Latvia*

Received 24 February 2000; accepted 28 June 2000

Abstract

We report the observation of the vibrational dependence of dissociative charge transfer (DCT), $Na_2(X^1\Sigma_g^+, v'') + Na^{**}(nl) \rightarrow Na^- + Na + Na^+$, in a single Na/Na_2 supersonic beam at low intrabeam collision energies (1.6 meV) using the STIRAP technique for selective vibrational excitation of Na_2 in the electronic ground state and time-of-flight mass analysis of the ions. The efficiency of this process increases by about an order of magnitude in the range $13 \leq v'' \leq 22$. Some perspectives are discussed regarding the implementation of a field-free ion-imaging technique for the detection of ions that will allow the direct determination of the kinetic energy distributions of product negative ions and thus distinguish among different possible mechanisms of the DCT process. The first results of test experiments on imaging of photodissociation products of $Na_2(v'')$ without an extraction field are presented, confirming the potential of the new detection concept. (Int J Mass Spectrom 205 (2001) 233–242) © 2001 Elsevier Science B.V.

Keywords: Dissociative charge transfer; Rydberg atoms

1. Introduction

Collisions of low-energy electrons with molecules have long been recognized as important elementary processes in plasmas [1]. Over decades, electron scattering experiments have been performed on various targets with ever-increasing electron energy resolution, recently down to the μeV range ([2,3] and references therein). The use of Rydberg atoms offers an alternative possibility to study low-energy electron scattering. In processes involving collisions with Rydberg atoms with high principal quantum numbers n, the large separation of the electron from the ion core allows one to treat the Rydberg electron as a nearly free particle. Detailed studies showed that for $l \ll n$, formation of negative ionic fragments by charge transfer from Rydberg states is very similar to the process of attachment of free electrons with the mean kinetic energy equal to a fraction (1/3–1/6) of their binding energy [4].

Dissociative attachment of free low-energy electrons to Na_2 molecules in the electronic ground state is known to depend not only on the electron energy but also on the vibrational level of the molecule [5–7].

* Corresponding author. E-mail: ekers@physik.uni-kl.de

Dedicated to Professor Aleksandar Stamatovic on the occasion of his 60th birthday.

PII S1387-3806(00)00290-6

This dependence is ascribed to the formation of Na_2^- in the repulsive $A^2\Sigma_g^+$ state with vibrational level–dependent coupling to the Na_2 ground electronic $X^1\Sigma_g^+$ state, followed either by the emission of the electron or by the fragmentation

$$Na_2(X^1\Sigma_g^+, v'') + e \rightarrow Na_2^-(A^2\Sigma_g^+) \rightarrow \begin{cases} Na_2(X^1\Sigma_g^+, v^*) + e, & (1a) \\ Na^- + Na, & (1b) \end{cases}$$

with the branching ratio between the channels strongly dependent on v″. One might also expect similar dependence on the vibrational level when the free electrons are replaced by weakly bound Rydberg electrons of Na**(nl) atoms. However, additional energy will be needed to ionize the Rydberg atom and to remove the negative ion from the ionic core of the atom.[1] Dissociative charge transfer (DCT) processes involving various molecular and cluster targets have been studied by several groups ([2,4,8–14] and references therein). To the best of our knowledge, no previous observation of the vibrational dependence of DCT has been reported in the literature.

The DCT process can proceed via two different mechanisms:

$$Na_2(X^1\Sigma_g^+, v'') + Na^{**}(nl) \rightarrow \begin{cases} Na_2^-(A^2\Sigma_g^+) + Na^+ \rightarrow Na^- + Na + Na^+, & (2a) \\ Na_3^{**} \rightarrow Na^- + Na + Na^+. & (2b) \end{cases}$$

Mechanism (2a) is the above-mentioned attachment of the weakly bound Rydberg electron. The electron is considered to be quasi-free, with the kinetic energy equal to its classical kinetic energy in the Rydberg orbit [2,4]. The electron attaches through vibrational level–dependent coupling to Na_2 in the $X^1\Sigma_g^+$, v″ state to form a temporary negative Na_2^- ion in the dissociative $A^2\Sigma_g^+$ state. Formation of such a temporary negative ion state, also called resonance, in collisions with electrons is well known and described in detail in, for example, [21–23]. The newly formed Na_2^- resonance may decay by electron emission yielding a neutral Na_2 molecule in a vibrationally excited state. If, however, the Na_2^- internuclear distance increases beyond the crossing point of the neutral and the resonance curves (see Fig. 1) before the electron is emitted, the dissociation of the molecular ion into stable Na^- + Na products is irreversible. A fraction of the Na^- kinetic energy is needed to overcome the Coulomb potential caused by the adjacent Rydberg core ion. The process may, however, be complicated by its three-body nature and the transient formation of a highly excited Na_3^{**} collision complex [mechanism (2b)]. The relevance of a Na_3^{**} complex in such a collision process is evidenced by the recent observations of the vibrational level dependence of the formation of Na_3^+ ions in associative ionization of excited sodium atoms and dimers [24,25].

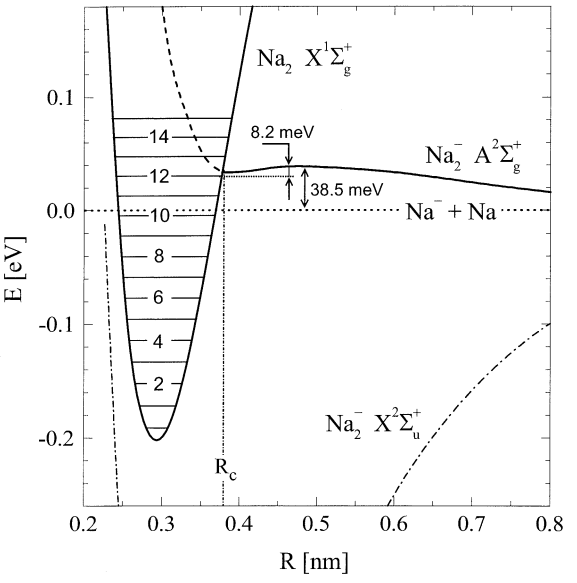

Fig. 1. $Na_2(X^1\Sigma_g^+)$ and $Na_2^-(A^2\Sigma_g^+)$ potential curves in the vicinity of the crossing point (adopted from [7]). The maximum of the broad barrier in the $A^2\Sigma_g^+$ state is 38.5 meV above the Na^- + Na asymptote, and 8.2 meV above the level v″ = 12, J″ = 9 of the $X^1\Sigma_g^+$ state [7]. The vibrational levels of the $X^1\Sigma_g^+$ state are correspondingly marked in the potential.

In this study, we are concerned with the formation

[1] Besides the ionization at the expense of the kinetic energy, the Rydberg electrons can be removed from the core through rotational [15–18] or vibrational [19] energy transfer or at the expense of electron affinity to the target molecules ([2,20] and references therein). The latter process leads to the formation of negatively charged atomic or molecular fragments.

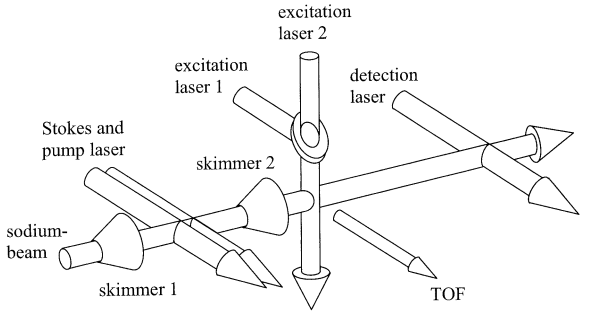

Fig. 2. Schematic arrangement of particle and laser beams. Excitation lasers 1 and 2 excite Rydberg atoms in the reaction region. The pump and Stokes lasers are used to implement STIRAP for the vibrational excitation of the dimers. The probe laser detects the vibrational excitation of the Na_2 molecules.

of negative ions in $Na_2(X^1\Sigma_g^+, v'') + Na^{**}(nl)$ collisions, in particular with the effect of vibrational excitation of Na_2 on the efficiency of negative ion formation. At present we cannot distinguish among the mechanisms (2a) and (2b). However, we present relevant data and discuss (in Section 4) the perspective of a future experiment, which will allow the determination of the kinetic energy distributions of the product ions. On the basis of such data we should be in a position to gain more detailed insight into the process. We also show results of first test experiments using that technique for a preliminary study of the photodissociation of $Na_2(v'')$.

2. The experiment

2.1. The supersonic beam setup

The experiment was performed with a single supersonic beam setup (see Fig. 2). We used a vacuum system with three differentially pumped chambers containing a supersonic beam source, a region for vibrational preparation of the molecules, and a reaction region with a time-of-flight mass analyzer, respectively.

The sodium beam source is operated at a temperature of 900 K. After expansion through a 0.4-mm-diameter nozzle, the temperature of which is held 50 K above the oven temperature, the beam is collimated by two skimmers (2 and 1.5 mm in diameter) 2 and 8 cm downstream from the nozzle opening and an entrance opening of the reaction region (3 mm in diameter) 18 cm downstream from the nozzle.

Under the present conditions, the densities of atoms and dimers in the reaction region are 2×10^{11} cm^{-3} and 2×10^{10} cm^{-3}, respectively. The following parameters of the beam were measured using laser-induced fluorescence and Doppler-shift techniques [26,27]. We found that 99% of the molecules are in the lowest vibrational level $v'' = 0$, with a maximum of the population distribution over rotational levels at $J'' = 7$. The mean particle velocity in the beam is 1340 m/s. The half widths at $1/e$ of the velocity distribution of atoms and molecules were determined as $\alpha_A = 150$ m/s and $\alpha_M = 130$ m/s, respectively. This yields the mean molecule-atom collision energy $\bar{E}_{MA} = \frac{1}{4}\mu(\alpha_A^2 + \alpha_M^2) = 1.6$ meV [28], where μ denotes the reduced mass.

2.2. Optical preparation of collision partners

Five laser beams cross the particle beam perpendicular to its axis (Fig. 2). The atoms in Rydberg levels *ns*, *nd* are excited in two steps in the reaction region. In the first step, a single-mode cw dye laser (CR-699-21, 1 MHz linewidth, Rh6G dye) radiation drives the $3s_{1/2} \rightarrow 3p_{3/2}$ transition (see Fig. 3a). To reduce the problem of optical pumping of atoms to the $F'' = 1$ level of the electronic ground state, the laser frequency is tuned to the $F'' = 2 \rightarrow F' = 3$ transition. Excitation and emission thus occur in a (nearly) closed two-level system, as spontaneous decay on the $F' = 3 \rightarrow F'' = 1$ transition is forbidden. The neighboring hyperfine levels $F' = 1$, 2 in the $3p_{3/2}$ state are only weakly excited through the wings of their absorption profiles. Weak optical pumping results from this excitation. It does not, however, influence the measured relative ion signal intensities, as the laser power was kept constant during the experiments. The second excitation step to Rydberg levels is achieved by means of the frequency-doubled radiation of a mode-locked Titanium: Sapphire laser (Coherent MIRA-900-P, 76 MHz rep. rate, pulse width $\tau \sim 3$ ps).

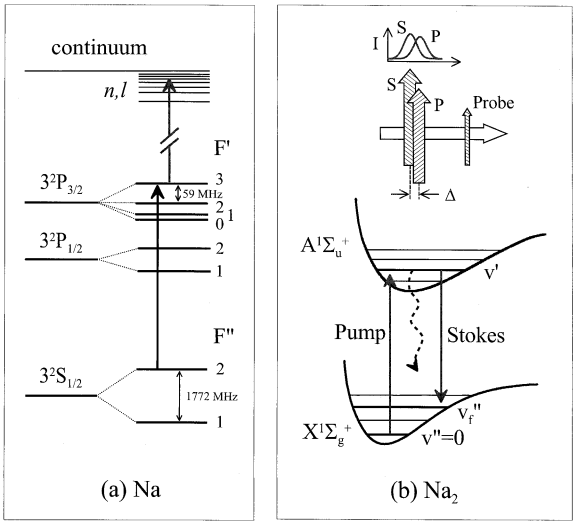

Fig. 3. (a) Excitation scheme of Rydberg atoms. Na atoms are excited from the $F'' = 2$ hyperfine sublevel of the ground $3^2s_{1/2}$ state predominantly to the $F' = 3$ sublevel of the $3^2p_{3/2}$ state. The second laser excites atoms from $3p_{3/2}$ to Rydberg *ns*, *nd* states. (b) Schematic presentation of STIRAP technique. A Stokes laser field (S) couples the intermediate state v' with the chosen final state v''_f before interaction of the molecules with the pump laser field (P). The correct sequence of laser pulses is adjusted by a proper shift Δ of the axis of the S and P laser beams. The efficiency of STIRAP is determined from the fluorescence signal induced by the probe laser (Probe).

The $3s \rightarrow 3p$ excitation laser is switched on for 1 μs by means of an acousto-optical modulator at a repetition rate of 100 kHz. After the excitation pulse, the reaction is allowed to proceed for 0.2 μs, after which a 1-μs-long 100 V/cm electric field pulse is applied that extracts the ions from the reaction region into the mass analyzer.

As the purpose of this work is to investigate the dependence of the efficiency of DCT on the vibrational excitation of the dimers, selective transfer of dimers to single vibrational levels of the electronic ground state is crucial. Such excitation is efficiently achieved by means of the stimulated Raman adiabatic passage (STIRAP) technique [29,30], which differs from the method of stimulated emission pumping [31,32]. In STIRAP a Stokes laser field (CR-899-Ti: Sa, 1 MHz line width) couples an intermediate (v', 10) level in the $A^1\Sigma_u^+$ state with the final (v''_f, 9) level in the electronic ground state before a pump laser field (CR-699-21, DCM dye, 1 MHz linewidth) couples the initial (0, 9) with the intermediate state (see Fig. 3b). The Stokes and pump laser beams cross the molecular beam at right angles. To ensure the correct sequence of laser pulses, the Stokes laser beam axis crosses the particle beam slightly upstream from the pump laser beam (see Figs. 2, 3b). Both laser frequencies are detuned off resonance from the respective one-photon molecular transitions by an equal amount of 100 MHz, maintaining the two-photon resonance for the transition ($v'' = 0$, $J'' = 9 \rightarrow v'$, $J' = 10 \rightarrow v''_f$, $J''_f = 9$). The vibrational excitation is monitored by measuring the fluorescence signal induced by a probe laser on the $A^1\Sigma_u^+(v'_{pr}, 10) \leftarrow X^1\Sigma_g^+(v''_f, 9)$ transition downstream from the reaction region.

3. Results and discussion

Figure 4 shows the experimental Na^- ion signals due to DCT as a function of the binding energy $E(nl)$ of the Rydberg electron and for the selectively excited vibrational levels $v''_f = 13$, 14 and 22 of Na_2. The Na^- signals are normalized to the photon flux of the $3p \rightarrow nl$ excitation laser. The $3s \rightarrow 3p$ excitation was kept constant during the measurements. The signal in the range -7.6 meV $\leq E(nl) \leq 0$ meV is not analyzed here because of an ill-defined contribution caused by electrons ionized out of high Rydberg states by the extraction pulse. For the given extraction voltage (100 V/cm), field ionization of Na**(nl) is possible for binding energies $|E(nl)| \leq 7.6$ meV [33]. For levels with a binding energy of $|E(nl)| > 7.6$ meV, the vibrational level dependence of DCT is reliably monitored.

We address one more feature seen in Fig. 4a–c. In all three figures, a marked peak is observed in the Na^- signal for high Rydberg levels close to the Na ionization threshold. We relate it to field ionization of Rydberg atoms by the extraction pulse. The field ionization of atoms in high-lying Rydberg levels creates free electrons. These electrons can dissociatively attach to the $Na_2(v'')$ for all three vibrational levels considered here, thus yielding Na^- ions in addition to those caused by the DCT process. The

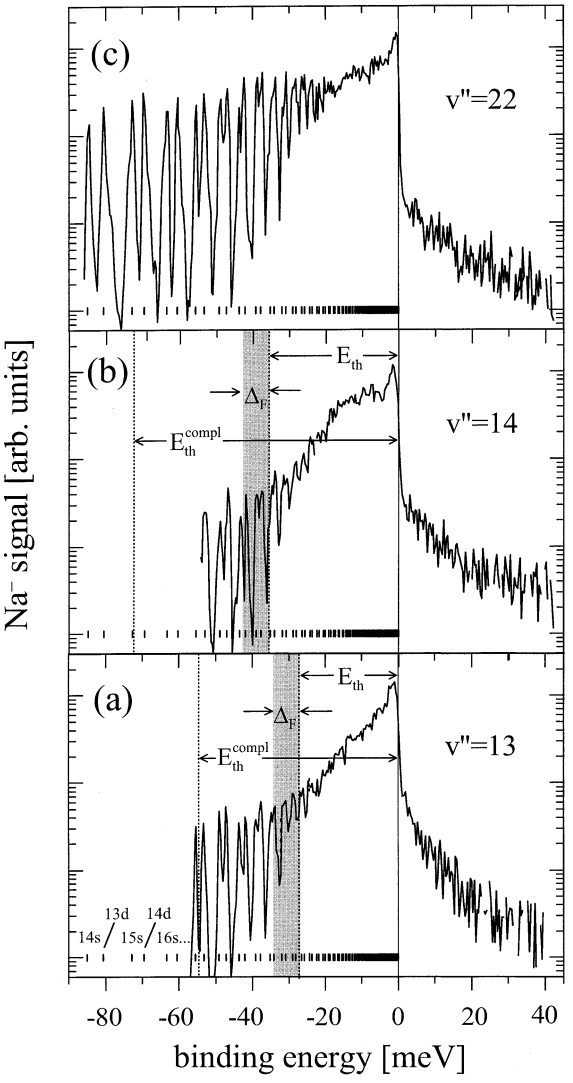

Fig. 4. Na^- ion signal caused by DCT as a function of binding energy of the Rydberg electron for three vibrational levels of Na_2: (a) $v'' = 13$, (b) $v'' = 14$, and (c) $v'' = 22$. Positive binding energies correspond to the attachment of low-energy photoelectrons to $Na_2(v'')$. E_{th} and E_{th}^{compl} denote the limiting binding energies of Rydberg electron for which the DCT is still possible according to quasi-free electron and Na_3^{**} complex models, respectively (for $v'' = 22$, $E_{th} = 101$ meV lies outside the scale of the figure). The shaded area of width Δ_F marks the lowering of Na ionization potential by the extraction field pulse.

Na^- signal in the region of positive electron energies is caused by the process (1b) of dissociative attachment (DA) of free photoelectrons to the dimers, which is studied in detail in [6,7].

Negative ions were only observed when the atoms were excited to the Rydberg state and, at the same time, the molecules excited to $v'' \geq 13$. As vibrational excitation of the molecules is essential for Na^- formation, we can rule out atomic pair transformation in Na($3s$, $3p$, or nl) + Na**(nl) collisions as a main source of atomic negative ions. At first glance, this conclusion seems to contradict the observations by Ciocca et al. [34], who observed the formation of Na^- for $n \geq 20$ in thermal collisions involving two Rydberg Na**(nl) atoms. They concluded that the negative ions result from the ion pair formation process Na** + Na** $\rightarrow Na^+ + Na^-$, which is exothermic by >5 eV. At low $n \geq 7$, a linear dependence of the Na^- signal on the density of Na**(nl) was observed and Na($3s$) + Na**(ns, nd) collisions were put forward as a source of negative ions. This interpretation ought to be reconsidered for the following reasons. Various experimental and theoretical studies of atomic ion pair formation have shown that this kind of process exhibits a resonant behavior for a total energy near or below the asymptotic energy of the ion pair state [35–37]. At large excess energies the process is not expected to proceed with a notable efficiency. The strong long-range attraction of the ion pair state prevents a curve crossing with covalent states, except possibly for small internuclear distances near the turning point of the radial motion. This is true because asymptotically the ion pair state lies >5 eV below the covalent ones in the case of Na** + Na** collisions and >0.25 eV in the case of Na($3s$) + Na**(nl). In addition, studies of associative ionization in Na($3s$) + Na**(np) collisions [38,39] (where, in contrast to [34] no intermediate $3p$ state was involved in the excitation of Rydberg levels) revealed no evidence of Na^+ ions at low n. This latter observation confirms that ion pair formation processes are unlikely to make a significant contribution. Indeed, our results suggest a different explanation of the observations reported in [34]. Their experiment was performed in sodium vapor; hence, vibrationally excited sodium dimers were present, with densities of 10^6–10^7 cm^{-3} in the levels $v'' \geq 13$. Furthermore, mutual collisions of Rydberg atoms lead to efficient Penning ionization with cross sections exceeding the

respective geometric ones [40,41]. Associative and Penning ionization in Na($3s$, $3p$, or nl) + Na**(nl) collisions also contribute to the free-electron production. The free electrons produced by Penning and associative ionization can interact efficiently with vibrationally excited dimers in the vapor, leading to the formation of Na^- through the DA process (1b). In addition, the Na^- ions can also be produced directly in collisions of Rydberg atoms with vibrationally excited dimers in the DCT process (2a) and (2b).

The large difference in the absolute Na^- signals in Fig. 4 resulting from DCT on one hand or from the attachment of free electrons on the other hand does not reflect a corresponding difference in rate coefficients. Rather it results from the much higher density of Rydberg atoms as compared to the density of free electrons. Photoelectrons leave the beam quickly, whereas long-lived Rydberg atoms travel in the beam along with vibrationally excited molecules. They may react for as long as 1.2 μs for the period between the beginning of the laser excitation and the electric field extraction pulse.

It is important to note that excitation of Na_2 to $v'' = 12$ yields very weak Na^- signals as compared to excitation of $v'' = 13$, 14, or 22. This can be understood from Fig. 1. The Na_2^- resonance $A^2\Sigma_g^+$ curve crosses the Na_2 $X^1\Sigma_g^+$ curve slightly above $v'' = 12$ at $R_c = 0.38$ nm. Furthermore, a broad maximum in the $A^2\Sigma_g^+$ curve around $R \approx 0.5$ nm rises 8.2 meV above the level $v'' = 12$, $J'' = 9$ populated in the experiment and hinders the dissociation [7]. The levels $v'' \geq 13$ are above the barrier of the $A^2\Sigma_g^+$ curve, so that all molecules are able to dissociate to Na^- + Na.

Another important feature is the increase of ionization efficiency for lower Rydberg levels as the vibrational excitation is increased from $v'' = 13$ to 22. The higher the vibrational excitation of the dimer, the more strongly bound Rydberg levels participate in the DCT. The shaded band in Fig. 4a and 4b corresponds to the limiting value of binding energy E_{th}, for which the DCT is still possible according to the quasi-free electron model (in Fig. 4c it is equal to 101 meV and lies outside the range of the figure). For high enough vibrational excitation, the dissociation of Na_2^- is much faster than the motion of Na_2^- in the Coulomb potential of the core ion. The threshold energy can be estimated from asymptotic energy considerations, assuming that energy released during the dissociation of Na_2^- is transferred equally to the translational energy of both dissociation products Na^- and Na, whereby Na^- has to overcome the Coulomb potential of the Na^+ core of the ionized Rydberg atom[2]

$$E_{kin}(Na^-) = \tfrac{1}{2}(E(v'') - D_e + E_{EA}) - |E(nl)|. \quad (3)$$

Here, $E_{kin}(Na^-)$ is the kinetic energy of the released Na^- ions, $E(v'')$ denotes the energy of vibrational excitation of the sodium dimer, D_e is the dissociation energy of the $X^1\Sigma_g^+$ state, and E_{EA} is the electron affinity of the Na atom. Setting in Eq. (3) $E_{kin}(Na^-) = 0$, we obtain for the threshold binding energy

$$E_{th} = \tfrac{1}{2}(E(v'') - D_e + E_{EA}). \quad (4)$$

Only Rydberg electrons with a binding energies $|E(nl)| < E_{th} + \Delta_F$ can participate in the DCT. The uncertainty Δ_F of E_{th} caused by lowering of the Na ionization potential by the 100 V/cm extraction pulse is 7.6 meV.

The observations are, however, not fully consistent with the quasi-free electron model. A rapid decrease in the Na^- signal at binding energies $|E(nl)| \leq 20$ meV for $v'' = 13$ as compared to plateau seen in the case of $v'' = 14$ may be an indication of the three-body nature of the DCT process. The $v'' = 13$ level lies just above the barrier of the $Na_2^-(A^2\Sigma_g^+)$ state. The dissociation for this level will proceed significantly slower than for $v'' > 13$. The interaction with the core ion is more likely to be important and may

[2] Strictly speaking, one has to account for the influence of the Na^+ core ion on the dissociation process of the Na_2^- ion. The Na_2^- ion can be accelerated or decelerated by the Coulomb potential of the core ion before and during the dissociation. The neutral Na product experiences the ionic core only through the much weaker (short-range) polarization potential. The kinetic energy of the Na^- ion required to escape from the Na^+ core depends on the Na^--Na^+ distance at the moment of dissociation. An estimate shows that the related uncertainty of the total required energy does not exceed a few meV. Therefore, we disregard the Coulomb interaction in Eq. (3).

lead to, for example, neutralization of the Na^--Na^+ pair and, thus, to a reduced efficiency of the ionization.

A Na^- signal is also observed for Rydberg levels below the threshold energy E_{th} (Fig. 4a, b). Since we did not observe any noticeable Na^- signal caused by excitation of Rydberg atoms only, vibrationally excited molecules are involved in the formation of Na^- also in this case. Equation (4) is not valid for the other possible mechanism (2b) of the DCT process, which assumes the formation of a highly excited autoionizing Na_3^{**} complex. That complex can dissociate into $Na^- + Na + Na^+$ through nonadiabatic coupling between the covalent and ionic potential energy surfaces correlating with the $Na_2(X^1\Sigma_g^+, v'') + Na^{**}(n, l)$ and $Na^- + Na + Na^+$ states, respectively. (Dissociation of the Na_3^{**} complex into $Na_2^+ + Na^-$ is energetically also possible. However, because of the large excess energy of 1 eV of this dissociation channel, similar considerations as those presented above for the case of the atomic ion pair formation also apply here, and the channel is expected to be inefficient.) Instead of condition (4), the asymptotic threshold energy in the case of the Na_3^{**} complex is given by

$$E_{th}^{compl} = E(v'') - D_e + E_{EA}. \quad (5)$$

The relation $|E(nl)| \leq E_{th}^{compl}$ is valid for low enough nl levels to explain the observations. Unfortunately there is not sufficient information available on the potential surfaces of Na_3^{**} correlating with $Na_2(X^1\Sigma_g^+, v'') + Na^{**}(nl)$ and $Na^- + Na + Na^+$ to allow unambiguous conclusions about further details of the process.

In summary, the data of Fig. 4 provide evidence that Na^- formation in the DCT process does not exclusively proceed via mechanism (2a), which can be treated by the quasi-free electron model. We do observe Na^- formation by DCT also for Rydberg levels that are sufficiently strongly bound to prohibit DCT according to Eq. (4a). Unambigious identification of the reaction mechanism may be based on the energy analysis of the Na^- fragments. Such energy analysis is, however, not possible with the time-of-flight setup used here. It will be possible with the scheme, discussed in the next section.

4. Novel field-free detection technique to study DCT

4.1. The principle and setup

We distinguish among the Na^- ions produced through process (2a) and (2b). From the above discussion it is clear that, according to the quasi-free electron model, the Na^- products will have (except for small corrections because of Coulomb interaction in the exit channel) a well-defined kinetic energy, determined by Eq. (3). In the case of Na_3^{**} complex formation, the transitions from the covalent to the ionic surface will take place at smaller internuclear distances, resulting in stronger Coulomb attractions compared with the quasi-free electron model. Therefore one would expect for mechanism (2b) lower kinetic energies and broader energy distributions of Na^-.

The new detection technique allows kinetic energy resolution of the ions. In addition, it results in a simplification of the experiment, as the STIRAP method for vibrational excitation of dimers can be replaced by the relatively simple Franck-Condon pumping (FCP) technique [32,42] that creates a distribution over vibrational levels in the electronic ground state. The ion signals caused by different v'' levels could be resolved as the kinetic energies of the ions will depend on v''. Furthermore, the technique does not require extraction fields in the collision region. Therefore, field ionization is avoided.

The idea is to use a modified version of the ion-imaging technique. The DCT process takes place at time t_0 in a small reaction volume located at $\vec{z}_r$ on the beam axis within a field free area (see Fig. 5). The velocity $\vec{v}_{ion}$ of the product ions is $\vec{v}_{ion} = \vec{v}_{beam} + \vec{v}_{DCT}(v'')$, where $\vec{v}_{beam}$ is the flow velocity of the particles in the beam and $\vec{v}_{DCT}(v'')$ the additional velocity gained in the DCT process.

The tip of the velocity vectors of the particles form a sphere (the so-called Newton sphere), the center $\vec{x}_c$

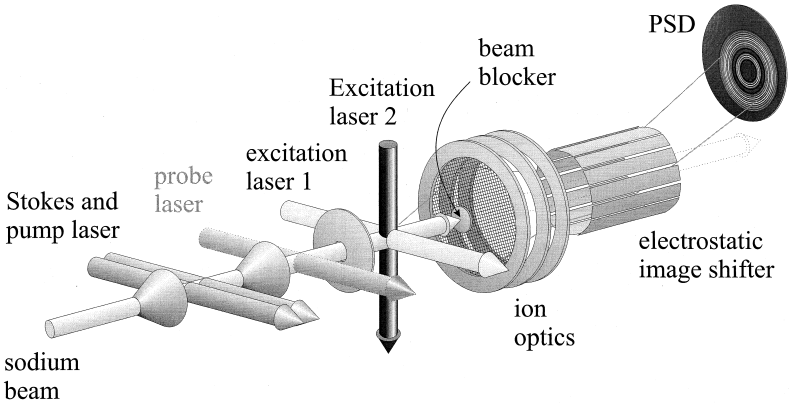

Fig. 5. Experimental setup for ion imaging without an extraction field. Compared to Fig. 2, the probe laser is moved upstream from the reaction region. Its operation is synchronized with the ion detection so that ions are registered when the probe laser is shut off. The beam blocker stops the beam and limits mechanically the reaction region before the entrance mesh of the ion optics. The electrostatic dodecapole image shifter displaces the ions focused by the ion optics onto the PSD.

of which propagates along the particle beam axis according to $\vec{x}_c = \vec{z}_r + \vec{v}_{beam}(t - t_0)$, while the radius R_N of the sphere expands as $R_N = |\vec{v}_{DCT}|(t - t_0)$. As soon as the ions have passed through the mesh (see Fig. 5) that separates the field-free region from the acceleration region, they are accelerated toward the position-sensitive detector (PSD). Usually, the detector is not gated (as no information on the arrival times is needed). Therefore, the sphere is projected onto the surface of the detector and yields two-dimensional (time-averaged) images of the spatial distribution of the ions in the vicinity of the mesh. Provided the distribution has axial symmetry, the three-dimensional information can be reconstructed [43,44] from this distribution.

The reaction chamber (not shown in Fig. 5) is formed by metallic plates with small openings for the lasers and a collimating 1.5-mm-diameter opening for the particle beam. The mesh separates the field-free reaction zone from ion optics that focuses the ions onto PSD (microchannel plates in Chevron arrangement followed by phosphor screen and CCD camera). The center of the PSD is displaced from the particle beam axis to prevent particles from the beam hitting the detector. The ions are accordingly displaced by a homogeneous electric field of a dodecapole image shifter (see [45,46] regarding application of multipole deflectors).

As both the vibrationally excited molecules and Rydberg atoms are in long-lived states, the reaction region is not restricted to the location where Rydberg atoms are excited but extends initially several centimeters downstream from the excitation site. We limit the reaction region by a mechanical 3-mm in diameter beam-blocker 20 mm downstream from the Rydberg excitation site. The distance between the blocker and excitation region was chosen to be large enough to allow the ions with low enough energies (down to 1.2 meV) to separate from the particle beam and pass the blocker into the ion optics. Such an extended reaction region results in a lowered energy resolution of the imaging (worse than the required $\leq$10 meV, which is about a half of vibrational level spacing of Na_2) if the system is operated in the space-mapping mode. The required resolution can be realized in the so-called velocity-mapping technique proposed in [47]. According to this technique, the potentials of the electrostatic lenses of ion optics are adjusted in such a way that ions with the same velocity component $v_{DCT,\perp}$ perpendicular to the beam axis are focused to a point on a ring with radius $r(v_{DCT,\perp})$ at the PSD regardless of the positions $\vec{z}_R$ where they are born.

4.2. Test using photodissociation of $Na_2(v'')$

Here we report results from first successful test of the setup using photodissociation of vibrationally

excited Na_2, a process that also yields atoms with well-defined kinetic energy. In these experiments, the pump laser vibrationally excites Na_2 to levels $v'' \geq 10$ in the electronic ground state by means of the FCP technique through the $A^1\Sigma_u^+$ state. The molecules in those vibrationally excited states are further photodissociated by the 457.9-nm Ar^+ laser line (excitation laser 1) through the $B^1\Pi_u$ state [48]:

$$Na_2(X^1\Sigma_g^+, v'') + h\nu_{Ar^+} \rightarrow Na_2^*(B^1\Pi_u) \rightarrow Na(3p_{3/2}) + Na(3s_{1/2}) + \Delta E(v'') \quad (6)$$

The $B^1\Pi_u$ state exhibits at large internuclear distances a potential barrier of 46 meV relative to the $3p_{3/2} + 3s_{1/2}$ asymptote [49]. The dissociation yields $Na(3p_{3/2})$ and $Na(3s_{1/2})$ atoms with well-defined kinetic energies, dependent on the vibrational level v'' of the molecule. Because of the barrier, we do not expect kinetic energies of the dissociation products <23 meV. The $Na(3p_{3/2})$ atoms are photoionized with the excitation laser 2 and detected with the ion-imaging detector. The polarity of the voltages has been changed for the detection of positive (rather than negative) ions. As the initial molecular population is distributed over levels v'', a distribution of kinetic energies is expected.

Figure 6 shows the two-dimensional velocity images of photodissociated $Na(3p_{3/2})$ products for two different intermediate levels $v' = 1$ (Fig. 6a) and $v' = 5$ (Fig. 6b) in the $A^1\Sigma_u^+$ state used for FCP. When $v' = 1$ is used, levels up to $v'' = 15$ are populated by spontaneous emission, while we have $v'' \leq 21$ for $v' = 5$. No signal is observed in the central part (corresponding to small kinetic energies) because the potential barrier of the $B^1\Pi_u$ state limits the smallest possible kinetic energy. Only a small fraction of that part is inaccessible to particles because of the finite size of the beam blocker. The first level that can be excited with 457.9-nm photons to energies above the barrier is $v'' = 10$. For that level the kinetic energy of the $Na(3p_{3/2})$ products is 30 meV. The larger size of the image in case of $v' = 5$ corresponds to the larger range of kinetic energies of the dissociation products. The contribution from individual vibrational levels of the dissociating molecules is not yet resolved. Therefore, we cannot draw further quantitative conclusions, as the photodissociation cross sections for individual v'' levels are not known. The resolution of the imaging detector depends sensitively on the adjustment of the voltages applied to ion optics and any stray electric fields that are present in the reaction chamber. Simulation studies taking into account the finite size of the reaction region and distortions of the electric field close to the surface of the mesh show that an energy resolution of an order of few meV can be achieved.

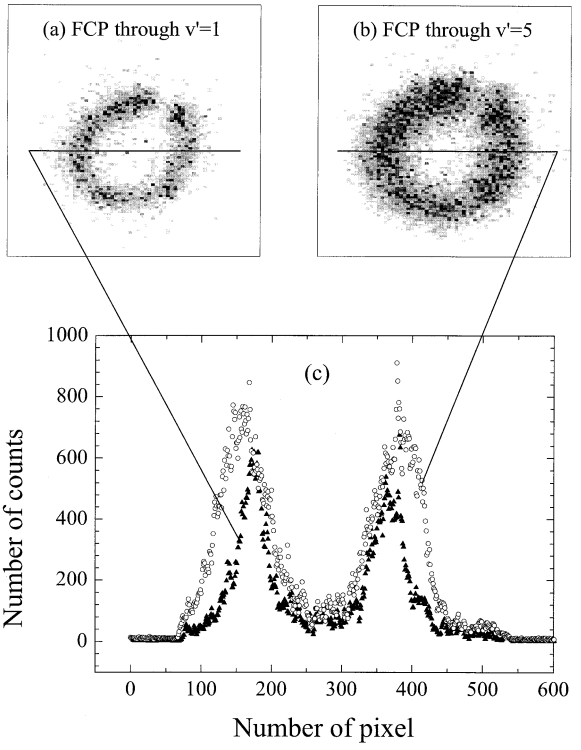

Fig. 6. Two-dimensional images of the photoionised $Na(3p_{3/2})$ products of photodisociation of $Na_2(v'')$ as obtained by imaging in the velocity-mapping mode. $Na_2(v'')$ are vibrationally excited by (a) FCP through $A^1\Sigma_u^+(1, 10)$ and (b) FCP through $A^1\Sigma_u^+(5, 10)$. The corresponding intensity profiles for cuts through the center of both images are shown in (c).

In conclusion, the efficiency of dissociative charge transfer in collisions of vibrationally excited $Na_2(v'')$ molecules with $Na^{**}(nl)$ Rydberg atoms depends on the level v''. Two mechanisms—the quasi-free electron and three-atomic collision complex models—

need to be invoked to rationalize the observations. A novel field-free ion imaging setup for the measurement of the kinetic energy distributions of product ions is described. The first test experiments show that different kinetic energy distributions of the ions can indeed be distinguished. Work is in progress to improve the energy resolution and to calibrate the setup using photodissociation of vibrationally excited Na_2.

Acknowledgments

This work is supported by the Deutsche Forschungsgemeinschaft. One of the authors (A.E.) is supported by the EU Marie Curie Individual Fellowship MCFI-1999-00368. We thank H. Hotop and W. Meyer for valuable discussions and L. Meyer for laser assistance.

References

[1] L.G. Christophorou, Electron Molecule Interactions and Their Applications, Vol. 2, Academic Press, Orlando, 1984.
[2] F.B. Dunning, J. Phys. B 28 (1995) 1645.
[3] A. Schramm, J.M. Weber, J. Kreil, D. Klar, M.-W. Ruf, H. Hotop, Phys. Rev. Lett. 81 (1998) 778.
[4] D. Klar, B. Mirbach, H.J. Korsch, M.-W. Ruf, H. Hotop, Z. Phys. D 31 (1994) 235.
[5] J.P. Ziesel, D. Teillet-Billy, L. Bouby, Chem. Phys. Lett. 123 (1985) 371.
[6] M. Külz, M. Keil, A. Kortyna, B. Schellhaaß, J. Hauck, K. Bergmann, W. Meyer, D. Weyh, Phys. Rev. A 53 (1996) 3324.
[7] M. Keil, T. Kolling, K. Bergmann, W. Meyer, Eur. Phys. J. D 7 (1999) 55.
[8] C. Desfrancois, N. Khelifa, A. Lisfi, J.P. Schermann, J. Chem. Phys. 96 (1992) 5009.
[9] H.S. Carman, Jr., C.E. Klots, R.N. Compton, J. Chem. Phys. 99 (1993) 1734.
[10] A. Pesnelle, M. Perdrix, J. Chem. Phys. 96 (1992) 4303.
[11] F. Misaizu, K. Mitsuke, T. Kondow, K. Kuchitsu, J. Chem. Phys. 94 (1991) 243.
[12] T. Kondow, J. Phys. Chem. 91 (1987) 1307.
[13] I.M. Beterov, N.V. Fateev, in: Himija Plazmy (Plasma Chemistry) Vol. 13, Energoatomizdat, Moscow, 1987, p. 40 (in Russian).
[14] T. Kraft, M.-W. Ruf, H. Hotop, Z. Phys. D 17 (1990) 37.
[15] X. Ling, K.A. Smith, F.B. Dunning, Phys. Rev. A 47 (1993) R1.
[16] X. Ling, M.T. Frey, K.A. Smith, F.B. Dunning, Phys. Rev. A 48 (1993) 1252.
[17] M.T. Frey, S.B. Hill, X. Ling, K.A. Smith, F.B. Dunning, Phys. Rev. A 50 (1994) 3124.
[18] C. Ronge, A. Pesnelle, M. Perdrix, G. Watel, Phys. Rev. A 38 (1988) 4552.
[19] M. Uematsu, K. Yamanouchi, T. Kondow, K. Kuchitsu, J. Chem. Phys. 85 (1984) 413.
[20] A. Pesnelle, C. Ronge, M. Perdrix, G. Watel, Phys. Rev. A 42 (1990) 273.
[21] J.N. Bardsley, A. Herzenberg, F. Mandl, Proc. Phys. Soc. 89 (1966) 321.
[22] J.N. Bardsley, F. Mandl, Rep. Prog. Phys. 31 (1968) 471.
[23] J.N. Bardsley, J.M. Wadehra, J. Chem. Phys. 78 (1983) 7227.
[24] A. Ekers, O. Kaufmann, M. Keil, K. Bergmann, Eur. Phys. J. D 7 (1999) 65.
[25] A. Ekers, O. Kaufmann, K. Bergmann, J. Alnis, J. Klavins, Chem. Phys. Lett. 304 (1999) 346.
[26] K. Bergmann, W. Demtröder, P. Hering, Appl. Phys. 8 (1975) 65.
[27] U. Hefter, K. Bergmann, in: G. Scoles (Ed.), Atomic and Molecular Beam Techniques, Vol. 1, Oxford University Press, New York, 1988, p. 193.
[28] H.M. Keller, M. Külz, R. Setzkorn, G.Z. He, K. Bergmann, J. Chem. Phys. 96 (1992) 8819.
[29] U. Gaubatz, P. Rudecki, S. Schiemann, K. Bergmann, J. Chem. Phys. 92 (1990) 5363.
[30] K. Bergmann, H. Theuer, B.W. Shore, Rev. Mod. Phys. 70 (1998) 1003.
[31] C. Kittrell, E. Abramson, J.L. Kinsey, S.A. McDonald, D.E. Reisner, R.W. Field, J. Chem. Phys. 75 (1981) 2056.
[32] K. Bergmann, in: G. Scoles (Ed.), Atomic and Molecular Beam Techniques, Vol. 1, Oxford University Press, New York, 1988, p. 293.
[33] T.F. Gallagher, Rydberg Atoms, Cambridge University Press, New York, 1994.
[34] M. Ciocca, M. Allegrini, E. Arimondo, C.E. Burkhardt, W.P. Garver, J.J. Leventhal, Phys. Rev. Lett. 7 (1986) 704.
[35] M. Reicherts, T. Roth, A. Gopalan, M.-W. Ruf, H. Hotop, C. Desfrancois, I.I. Fabrikant, Europhys. Lett. 40 (1997) 129.
[36] K.W. McLaughlin, D.W. Duquette, Phys. Rev. Lett. 72 (1994) 1176.
[37] I.I. Fabrikant, J. Phys. B 31 (1998) 2921.
[38] S.B. Zagrebin, A.V. Samson, J. Phys. B 18 (1985) L217.
[39] J. Boulmer, R. Bonanno, J. Weiner, J. Phys. B 16 (1983) 3015.
[40] C.E. Burkhardt, W.P. Garver, V.S. Kushawaha, J.J. Leventhal, Phys. Rev. A 30 (1984) 652.
[41] R.E. Olson, Phys. Rev. Lett. 43 (1979) 126.
[42] K. Bergmann, U. Hefter, J. Witt, J. Chem. Phys. 72 (1980) 4777.
[43] R.N. Strickland, D.W. Chandler, Appl. Opt. 30 (1991) 1811.
[44] D.W. Chandler, P.L. Houston, J. Chem. Phys. 87 (1987) 1445.
[45] N. Yonekura, C. Gebauer, H. Kohguchi, T. Suzuki, Rev. Sci. Instrum. 70 (1999) 3265.
[46] M. Szilagyi, Electron and Ion Optics, Plenum, New York, 1988.
[47] D.H. Parker, A.T.J.B. Eppink, J. Chem. Phys. 107 (1997) 2357.
[48] M.L. Janson, S.M. Papernov, J. Phys. B 15 (1982) 4175.
[49] E. Tiemann, Z. Phys. D 5 (1987) 77.